

# INTERFEROMETRY PROGRAM FLIGHT EXPERIMENT #1 : OBJECTIVES AND RESULTS.

M. Levine \*, R. Bruno\* and H. Gutierrez\*

•California Institute of Technology  
Jet Propulsion Laboratory  
4800 Oak Drive  
Pasadena, CA 91109

\*Massachusetts Institute of Technology  
Department of Astronautics and Aeronautics  
Cambridge, MA 02139

**ABSTRACT:** The *Interferometry Program Experiments (IPEX) I and II* are a series of flight experiments designed to characterize microdynamics of structures in space. Of particular interest is potential thermal snapping when space structures undergo rapid thermal variations, such as a sun-to-shade transition. This information is needed to characterize uncontrollable high frequency disturbances in future space interferometry missions. Both experiments are performed on the German DARA/DASA free-flying platform Astro-Spas, which is sorted out of the shuttle with the robot arm and retrieved after a 10-day mission. IPEX-I, performed during the STS-80 mission in December 1996, was a suite of 12 micro-g accelerometers which monitored the on-board dynamics of the Astro-Spas during normal operations and quiescent periods. The paper will report the results of the IPEX-I flight experiment. The paper will also describe the second flight experiment, IPEX-II, which will be performed during the STS-85 mission in August 1997, and will monitor the microdynamic behavior of an AEC-ABLE mast.

## 1. INTRODUCTION

NASA has selected the Jet Propulsion Laboratory (JPL) to be the lead center for new technology development in area of space optical interferometry. The Space Interferometry Mission (SIM) will be NASA's first space interferometer designed specifically for measuring the position of stars, and is scheduled for launch into low Earth orbit in 2005. SIM will utilize multiple 40-cm telescopes placed along a 10-meter (33-foot) long boom, as depicted in Figure 1. By measuring the "interference" of the light collected from these separate mirrors, SIM is able to make highly accurate position measurements. SIM can also produce pictures by combining the starlight gathered by those same special mirrors and by synthesizing an image comparable to that produced by a much larger telescope, for only a fraction of the cost.

One of the technologies that must be accomplished for SIM to meet its science requirements is the *nanometer* (10<sup>-9</sup> m) level stabilization up to 300Hz of the optical pathlength, on the lightweight 10-meter flexible structure, in the presence of spacecraft vibrations and transient thermal distortions. Most of the disturbances will be

attenuated through vibration isolation at the mechanical disturbance source (e.g., reaction wheels) and through high-bandwidth optical pathlength control of the delay lines and fast-steering mirrors. However, of concern are the quasi-random disturbances, such as thermally induced vibrations that are likely to occur when the spacecraft is subjected to large instantaneous temperature gradients. Also, for the vibration attenuation strategies to be successful it is necessary to have an *a-priori* knowledge of the vibration source characteristics, the propagation of these disturbances through out the structure, and the dynamic properties of the structure, in its zero-g operating conditions. These disturbance and structural models are required for integrated *opto-thermo-mechanical* disturbance prediction, instrument design, and science requirement verification.

However, little is actually known about the broadband microdynamic behavior of space structures on orbit. Data from the Hubble Space Telescope demonstrated the existence of thermally induced snapping [1]. Also, microgravity surveys were performed on orbiting space platforms, such as EURECA [2]. However, the objective of those measurements was to characterize the low-frequency behavior below 5Hz for verification of the microgravity science requirements.

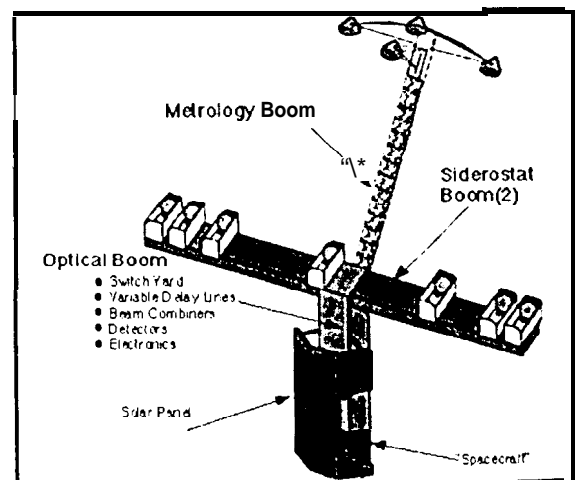
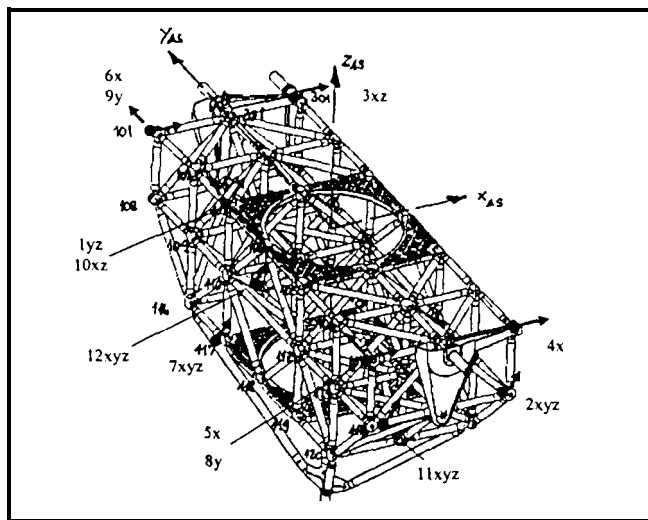


Figure 1 SIM Structural Design



**Figure 2. ASTRO-SPAS Frame with IPEX-I Accelerometer Locations**

The *Interferometry Program Experiments*, IPEX-I and IPEX-II, took advantage of two ASTRO-SPAS (Shuttle **P**allet Satellite) flights, scheduled off STS-80 (November 1996) and STS-85 (August 1997) to gain more knowledge on the broadband mechanical and thermal behavior of actual space structures on orbit. The reusable science satellite, ASTRO-SPAS (A/S), is a spacecraft developed by MBB Deutsche Aerospace, which is launched into Earth orbit by the Space Shuttle and deployed for a free flight period of approximately 10 days. At the end of its mission, the A/S is retrieved into the Shuttle and returned to Earth. The A/S is designed as the primary structure for precision optical instruments and can accommodate telescopes with dimensions up to 1.2m diameter and 3.9m length; additional small instruments can be mounted on the top or side of the pallet. The main structure of the A/S is roughly 4.6 ft x 14 ft x 2.3 ft, as shown in Figure 2. The total payload mass can reach 1800 kg, with an integrated satellite system mass of up to 3600 kg. The A/S is a low weight, high stiffness frame made out of carbon fiber compound tubes and titanium nodes, with standardized aluminum mounting panels for subsystem and payload equipment. Passive thermal control is achieved via radiation and conduction through multi-layer insulation blankets. The A/S has a 3-axis-stabilized gyroscope control system with precision star tracker as reference for pointing accuracy below 5 arcsec to astronomical targets. Twelve Nitrogen or Helium cold gas thrusters of 100 mN each are used for attitude control. Two thruster blocks are attached at the +Y and -Y ends of the structure as shown in Figure 2. The third is located at the keel under the platform. The thrusters apply a 100 mN pulse with a maximum duration of 200 msec and a minimum duration of 25 msec. The on-board attitude control systems automatically determines the pulsing direction and duration. A manual override exists, which allows the user to define the thruster firings for specific maneuvers. The A/S is powered by modular Li-SO<sub>2</sub> lithium battery pack of units of 10kWh each, for a total of 20 to 50 kWh for the payload depending on the mission duration. The flight data is directly recorded onto magnetic tapes, which is then retrieved and processed when the A/S returns to Earth.

The A/S is controlled from its own operations center at Kennedy Space Center (KSC) using the Shuttle as relay station for the command and the telemetry link.

NASA and the German Space Agency DARA GmbH have agreed to perform at least 4 joint missions with the A/S system. The third SPAS mission on STS-80, named "ORFEUS-SPAS" carried the German Ultraviolet telescope ORFEUS for hot star observations as the core payload, with the NASA/JPLIPEX-I as one of its Payload complement. IPEX-I characterized the vibrational environment of the A/S platform itself to determine whether it would meet the broadband nanometer stability requirements of a potential SIM technology demonstration flight. The last SPAS mission on STS-85, named "CRISTA-SPAS" carried the German CRISTA cryogenic spectrometer telescope for mapping of the Earth's upper atmosphere, with the NASA/JPLIPEX-II as one of its other payloads. During IPEX-II a nine-bay joint-dominated pre-loaded truss was cantilevered off the side of the CRISTA-SPAS and instrumented with accelerometers, load cells, thermistors and shakers for complete on-orbit dynamic and thermal characterization of a potential SIM structural element.

## 2. IPEX-I

### 2.1. Experiment Design and Objectives

IPEX-1 was designed to record the A/S accelerations during two orbits. The objective is to evaluate the structural response in normal operating conditions and during a prescribed quiet time when the thruster firings are stopped. Approximately 229 minutes of acceleration time histories from twelve micro-g accelerometers were analyzed and the data was used to:

- 1) observe the structural behavior as the A/S goes through sun and shade transitions and determine whether thermal snaps exist,
- 2) determine the effect of on-board mechanical disturbances identified in the flight log,
- 3) correlate disturbance levels to ground tests and finite element model predictions

The expected microdynamic disturbances are those induced by the gyros, flight data recorders (DAT) and the thruster mechanical relays. Of importance are also the thermally induced vibrations, a.k.a. "snap-crackle and pop". These may occur because of the mismatch in the coefficients of thermal expansion (CTE) between the graphite-epoxy frame, the titanium node connectors and the aluminum panels. The thermally induced vibrations will be monitored during periods of complete shutdown of the A/S.

The model used in the finite element analysis was provided by DASA, as shown in Fig. 2 with the twelve accelerometer locations and direction marked. The reduced order model has 55 nodes (one for each node ball in the frame structure) and 330 degrees of freedom which include the ORFEUS telescope and IMAPS telescope.

The micro-g accelerometers used were Sundstrand model QA-2000 sensors with a built-in temperature sensor. The data sampling system (DSS) provided 12-bits of accuracy, with a sampling rate of 745 Hz and a second-order anti-aliasing filter at 372.5 Hz. Eleven of the twelve sensors were calibrated to read 50 mg peak-to-peak and the twelfth was set at 1 g peak-to-peak. The sensor noise levels are approximately 9  $\mu\text{g}$  between DC and 10 Hz, and 80  $\mu\text{g}$  between 10 Hz and 500 Hz.

Data was successfully recorded for all twelve accelerometers from the IPEX-1 acquisition system. The 9  $\mu\text{g}$  to 50 mg window was sufficient to capture the on-orbit dynamics, since none of the recorded time histories appeared to be clipped or measuring bit noise. The largest acceleration recorded over all channels, except Channel 4, is less than 1.8 mg. Channel 4 is the only channel that had the 1 g resolution. After applying the calibration factors, the data from Channel 4 was at least an order of magnitude higher than any other channel, even those located near it. Since there is no logical explanation for this anomaly, it is suspected that the calibration scale wasn't set correctly for this channel, either in the flight hardware or software. Hence, the data from this channel will not be presented herein.

## 2.2. Flight Results

The flight data has been analyzed in detail in Ref. [3]. The main events of the first orbit include a quiet time during which the thrusters were continuously on, 1 day/night transition, and 1 night/day transition. The mechanical disturbances applied to the A/S during the first orbit include the gyros, the data recorders, the IMAPS telescope, and the thruster nozzles. The second orbit includes a 3-minute quiet period where the thrusters were intentionally inhibited, 1 day/night transition, and 1 night/day transition. The mechanical disturbances for the second orbit remain the same with the exception of the IMAPS telescope that was not operational. The environment during the quiet time represents the minimum noise floor without any thruster input. During this time, the measured response can be considered a stationary, ergodic random process and the response can be quantified in terms of acceleration RMS values, peak accelerations, PSD's, and residual motion.

### 2.2.a. Thruster and Gyro Activity

The dominant disturbance to the A/S platform is from the thruster firings. There are 3 sets of thruster assemblies located at each end of the structure and at the bottom of the keel. By comparing the thruster command log and the time of the event measured from the acceleration data, it was concluded that the disturbance resulted from the opening and closing of the mechanical valves on the nozzle, rather than from the acceleration due to the gas release. A sample of the measured accelerations is shown in Figure 3 for Channel 5, located at one end of the A/S and near a thruster assembly. The data includes 3-second time period where (a) the thrusters are turned off; (b) the thruster firings are more frequent, and (c) the thruster firings depict nominal operation modes.

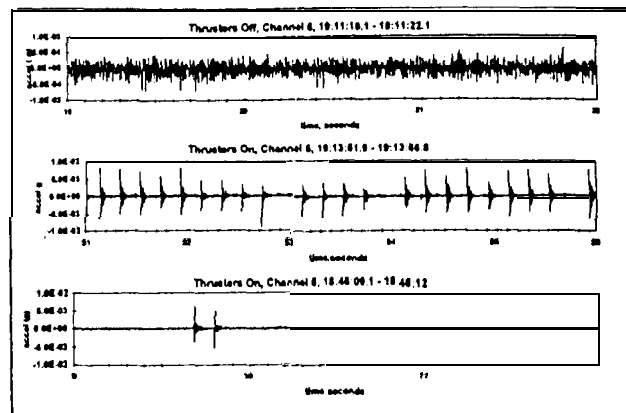


**Figure 3. Typical Acceleration at Channel 5: a) Quiet Period, b) High Thruster Activity, c) Nominal Activity**

The acceleration RMS values for the 3-second time period 19:09-19:12 during the second orbit when the thrusters were off are presented in Table 1, and shown in Figure 3a for Channel 5. The values presented in Table 2 are extracted from the time period 18:29-18:34 when the thrusters are on. This is one of two time periods when the thruster firings are more frequent and represent the upper bound disturbance level, as shown in Fig. 3b compared to a typical thruster firing sequence in Fig. 3c. During these two periods, the gyros and recorders were functioning and contributing to the background disturbances.

The RMS values for the discrete frequency bands are obtained by integrating the PSD curve. Hence, the computed RMS values may also be conservative because of aliasing. Disturbances above the IPEX-I flight system Nyquist frequency of 372.5 Hz will appear aliased at a lower frequency in the PSD's and will then be included in the integrated RMS values. In particular, the A/S ground test data presented in Ref. [3], and summarized in Table 3, identified gyro disturbances above 372.5 Hz. The gyro frequencies at 800 Hz and 500 Hz are believed to be aliased down to 55 Hz and 245 Hz, respectively, and are predominant in channels 1, 5, 8, and 10 (Fig. 4 and 5). These channel locations also coincide with those having the largest RMS disturbance values in the IPEX-I flight data (Table 1 and 2). To provide a more realistic set of RMS values, a second set was calculated in which the peaks from the gyros were removed. The PSD peaks were truncated down to the background level at 55 and 245 Hz and the RMS calculations were repeated.

With the aliased gyro contribution removed, the A/S disturbance levels with the thrusters off, are approximately 15  $\mu\text{g}$  RMS for [0-10] Hz, 40  $\mu\text{g}$  to 120  $\mu\text{g}$  RMS for [10-100] Hz, and 70  $\mu\text{g}$  to 140  $\mu\text{g}$  [100-372.5] Hz. The broadband RMS range from 80  $\mu\text{g}$  to 180  $\mu\text{g}$ . These numbers do not include Channels 1 and 10, which are collocated on the top of the spacecraft, next to the support panels for the Orfeus telescope. The PSD for Channel 1, shown in Fig. 5, displays large resonances

Ch	0-10 Hz		10-100 Hz		100-372.5 Hz		0-372.5 Hz	
	w/	w/o	w/	w/o	w/	w/o	w/	w/o
	gyro	gyro	gyro	gyro	gyro	gyro	gyro	gyro
1	18	18	303	254	273	273	406	373
2	14	14	47	43	76	75	90	86
3	14	14	47	46	60	79	93	93
5	14	14	117	109	141	141	184	179
6	16	16	54	53	90	90	106	106
7	15	15	115	53	86	67	145	103
8	16	16	66	70	126	125	153	145
9	13	13	42	40	73	72	85	84
10	20	20	162	109	197	197	256	226
11	15	15	48	47	100	100	112	112
12	14	14	46	44	62	62	95	94

Table 1. Astro-Spas On-Orbit Disturbance RMS with Thrusters Off, in units of  $\mu g$ .

Ch	0-10 Hz		10-100 Hz		100-372.5 Hz		0-372.5 Hz	
	w/	w/o	w/	w/o	w/	w/o	w/	w/o
	vro	vro	vro	vro	gyro	gyro	gyro	gyro
1	19	19	286	244	257	257	385	355
2	30	30	67	84	133	133	161	160
3	14	14	48	44	84	84	96	96
5	19	19	154	147	231	232	279	275
6	17	17	56	53	94	94	111	109
7	20	20	119	56	94	94	153	111
8	35	35	147	139	172	171	229	223
9	18	16	56	53	86	85	104	102
10	21	21	167	109	169	169	253	219
11	21	21	66	63	131	131	148	147
12	15	15	50	46	95	95	108	106

Table 2. Astro-Spas On-Orbit Disturbance RMS with Thrusters On, in units of  $\mu g$ .

between 150 Hz and 200 Hz, which do not appear in the other channels. Hence, the RMS values for the Channels 1 and 10 may be higher because of resonances in the adjacent support panels: approximately 20  $\mu g$  RMS for [0-10] Hz, 250  $\mu g$  RMS for [10-100] Hz, and 270  $\mu g$  for [100-372.5] Hz. The quietest Channels, 2, 3, 9, and 12 are approximately 90  $\mu g$  broadband for [0-372.5] Hz (Table 1).

The aliasing effects of the gyros are the greatest at Channel 7 where the RMS is increased by 60  $\mu g$  RMS for [10-100] Hz, and which is contributed by the gyro frequency at 800 Hz aliased down to 55 Hz (Tab.1, Fig. 6).

However, the thruster nozzles remain the most significant source of mechanical disturbances in the spacecraft, as is reflected by the increased RMS values between the

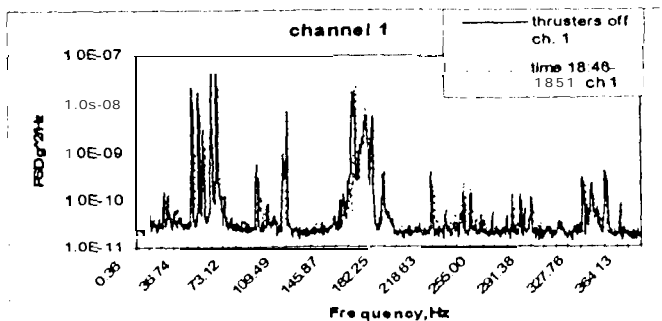


Figure 4. Typical PSD ( $g^2/hz$ ) at Channel 5, for thrusters-on and thrusters-off phases of the mission.

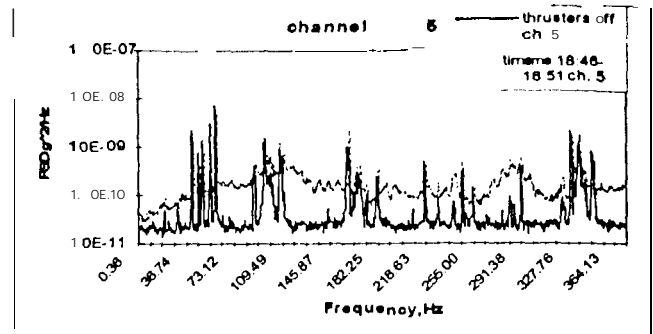


Figure 5. PSD ( $g^2/hz$ ) at Channel 1, for thrusters-on and thrusters-off phases of the mission.

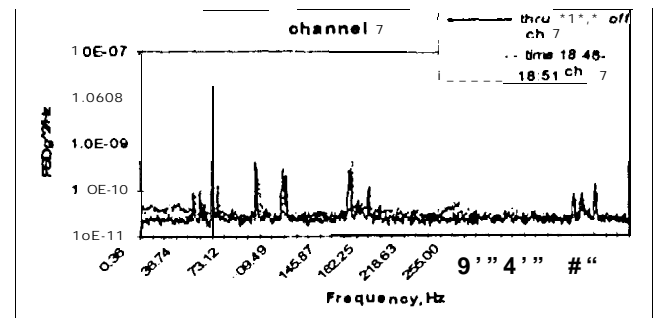


Figure 6. PSD ( $g^2/hz$ ) at Channel 7, for thrusters-on and thrusters-off phases of the mission.

thrusters off and on period (Table 1 and 2). This is especially true for Channels 5 and 8, which are located near the thruster nozzles, on the [-X-Y] corner of the spacecraft, and for which the broadband RMS has increased by approximately 100  $\mu g$ . This is also illustrated in Fig. 4, where the PSDs of Channel 5 during the thrusters on and off period are superimposed. Of course, computing a PSD for a transient signal is not mathematically correct since the pulsing sequence is neither random nor periodic in nature, however, it provides a visual representation of the frequency content of the disturbance. The thrusters impact the structure like an impulse, thus supplying a broadband excitation and increasing the broadband PSD floor level. Some of that increase in the noise floor may also be due to aliasing. Channels that are located away from the thruster assembly at the +Y end of the structure, such as Channel 3, 6, 7 and 9, did not display a significant change in the PSD (Fig. 7). Whereas, all channels located near the -Y end of the structure, such as channels 2, 5, 8, and 11 saw significant increases in the RMS levels. It is suspected that nonlinear mechanisms, such as joint friction and material damping, attenuate the propagation of the nozzle pulse along the structure.

The acceleration peak values, during normal operations, from orbits 1 and 2 are shown in Fig. 7. These were obtained by reading the full data set and extracting the maximum absolute value for each sensor and the time at which it occurs. The peaks occur when the thrusters are firing frequently. Peak accelerations in channels 1, 2, 7, 10, 11, 12 are relatively close in magnitude, while large

DISTURBANCE SOURCE	FREQUENCY	EFFECT ON BOOM
GYROS	505 Hz 800 Hz	0.2mg RMS added by 800 Hz spike to x-dir. response of boom tip
TAPE RECORDERS	>600 Hz	Negligible
THRUSTERS	Impulse	1 mgRMS at boom tip?
CRISTA TELESCOPE	>500 Hz	~0.1 mg RMS contribution to interface strut response (during grating operation)
MAHRSI TELESCOPE	Multiples Of 100Hz	0.2 mg RMS contribution to interface strut response

**Table 3. Summary of Mechanical Disturbances Observed During IPEX-II Ground Integration Tests [3].**

differences occur between the two orbits for the remaining channels at the top 4 corners of the A/S. As seen earlier, the structure appears to respond to the mechanical disturbance induced by the thruster nozzle opening and closing. The change of location for the peak accelerations could be explained if the z rotation was applied by +y end thrusters in Orbit 1 and the -y end thrusters in Orbit 2.

The peak accelerations for the quiet times of the two orbits are shown in Fig. 8. For the first orbit, the quiet time is defined as a period where the thrusters are continuously on rather than repeated pulsing. For the second orbit, the quiet time is the designated period of three minutes where the thrusters are turned off. With the exception of the

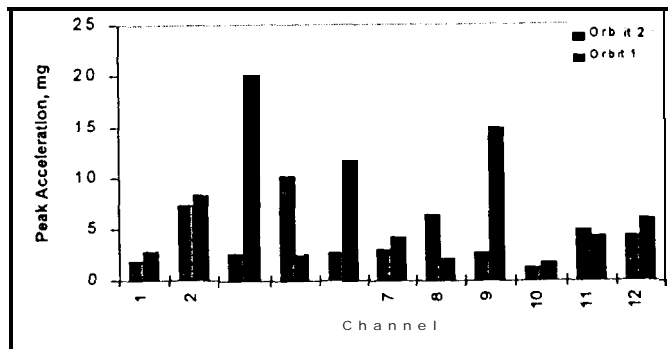


**Figure 7. Peak Accelerations during Normal Operations.**

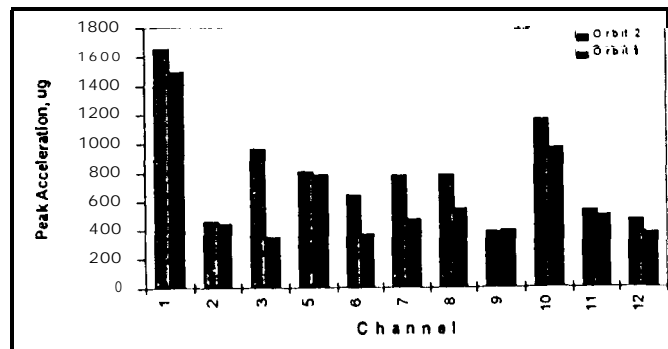


**Figure 8. Peak Accelerations during Quiet Mode.**

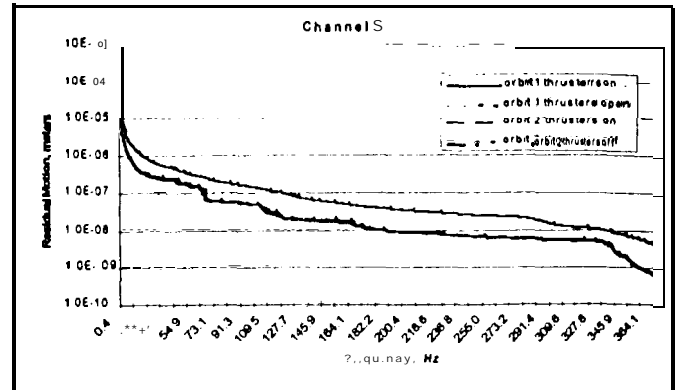


**Figure 9. Residual Motions at Channel 5 for Thrusters on and off conditions during Orbits 1 and 2.**

response from Channels 3 and 4, the peak values do not show significant differences between the two orbits. In fact, the peaks when the thrusters are continuously on are lower than when the thrusters are turned off at all measurement locations except number 9. The highest peak accelerations are recorded at Channels 1 and 10, which are almost unchanged from the thrusters-on condition. These are the collocated channels near the Orfeus mount plate.

Another way of characterizing flight data is with residual motion plots as shown in Fig. 9 for Channel 5. Residual motion is computed using the reverse cumulative displacement RMS and represents the necessary controller bandwidth to achieve the desired stability requirement. This information is important when designing structures with high stability requirements, such as SIM. The plots presented here are calculated for a period of time where the thrusters remain open in Orbit 1, a five minute period of normal operations in Orbit 1, the specified quiet time in Orbit 2, and a five minute period of normal operations in Orbit 2. In general, the response during the first orbit for normal operations is higher than in the second orbit, since the active thrusters were located closer to Channel 5. Figure 9 is interpreted by first identifying the desired level of stability in terms of displacement then reading the associated frequency, which represents the necessary controller bandwidth. Hence, a 300 Hz bandwidth controller would be needed during nominal thruster operations to attenuate the motion down to 10 nanometers, as required for SIM.

#### 2.2.b. Slewing Effect

The slewing maneuvers and transitions have no noticeable effect on the time histories. The only event that is clearly evident in the time histories is when the thrusters are turned off and on.

#### 2.2.c Day/Night Transitions

The sun transitions occur during the second orbit at 19:16 for the day/night transition and 19:51 for the night/day transition. Fig. 10 shows the response from Channel 5 for 10 seconds before and after the dayto<sub>night</sub> transition time. None of the channels show evidence of a thermally induced response or snapping when the platform moves into or out of complete shade.

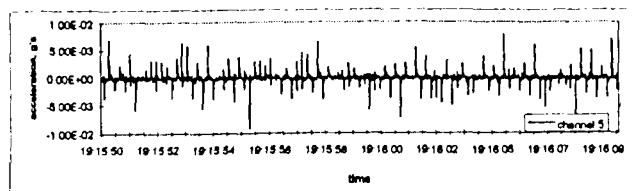


Figure 10. Acceleration Time History at Channel 5, during day/night Transition at 19:16.

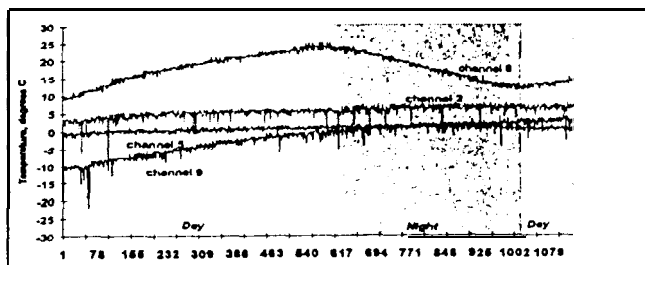


Figure 11. Temperature Time Histories at Channels 2, 5, 8, 9) during Sun Transitions.

A few representative temperature histories are plotted in Fig. 11. The sensors are collocated with the accelerometers, and positioned inside the accelerometer housing. The temperature at Sensors 2 and 9 display an overall gradual increase, which may indicate heat buildup from nearby electronics. The temperature at Sensor 8 increases during the day and decreases at night with an overall temperature variation of approximately 14°C. Unlike the others, this accelerometer is mounted outside the MLI blanket, thus the cyclic environmental temperature effects are more apparent.

#### 2.2.d. Anomaly in Channel 3

An impulse appears in Channel 3 at time 19:09:26 when the thrusters are turned off (Fig. 12). The acceleration shows a peak and decay ring down typical of a structural response to an impulse-like excitation. The magnitude is 2 mg peak-to-peak. It does not occur during a sun/shade transition or a sudden change in thermal environment. Also the IMAPS telescope was not operational during this recorded orbit. No other channels show a similar response at this time.

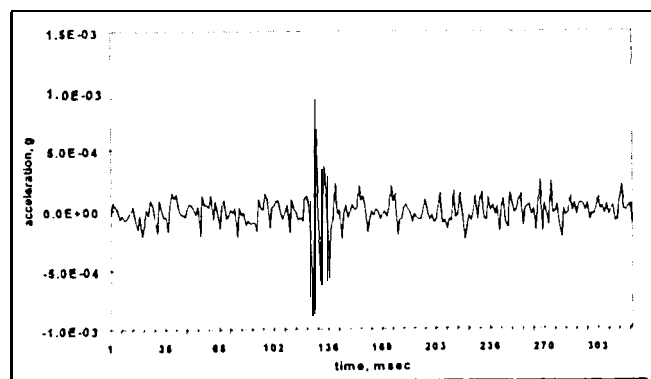


Figure 12. Anomalous Impulse at Channel 3.

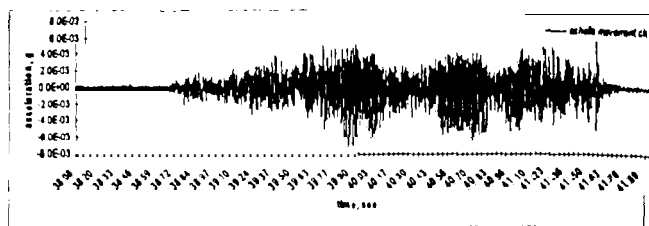


Figure 13. Acceleration Time History at Channel 3, during IMAPS Echelle Grating Motion.

#### 2.2.e. IMAPS Influence

The IMAPS telescope was operational during the first recorded orbit, day 334. The expected loading from IMAPS is due to movement of the echelle grating and the drive motor. The motor frequency has been loosely estimated at 130 Hz, but no measurements are available. The echelle grating can be tilted in four different positions and for a particular target, will remain in each position for anywhere from 40 seconds to several minutes.

The measured response on the A/S structure shows the disturbance from the motion of the echelle grating only on the first movement for acquisition of a new target. Fig. 13 shows the acceleration time response from Channel 3 when the grating is moving. During this time period shown, the thrusters are not active. The maximum response from the grating motion is approximately 7 mg. The PSDS from this time period show additional peaks at around 36 Hz, 200 Hz and 345 Hz, and could be due to the echelle grating motion. There is a possibility that these have been aliased down from a higher frequency.

#### 2.3. Astro-Spas Dynamic Identification

##### 2.3.a. Structural Damping

A damping coefficient is estimated by determining the rate of decay of free oscillations. Two time periods were selected when the thrusters are firing and the logarithmic decrement of successive peaks is used to calculate the damping factor. The damping is estimated at 1.2%.

##### 2.3.b. Measured Structural Modes

Time domain identification tool ERA was implemented for the purpose of extracting on-orbit modal properties of the AfS. However, the data extracted from this approach was not conclusive.

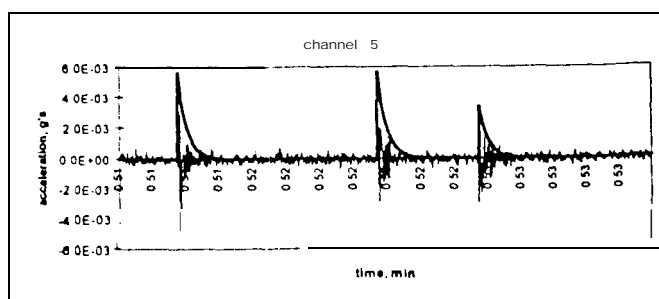
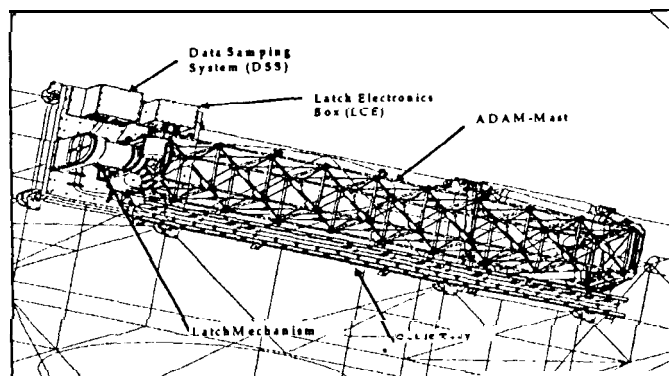


Figure 14. Decay Envelope with  $\zeta=1.2\%$  for Channel 5.

### 3. IPEX-II

The data obtained from IPEX-I was used to estimate the background disturbances for the follow-on flight experiment, IPEX-II, which was flown on STS-85 in August 1997. In IPEX-II, a 9-bay 2.3m x 0.3m x 0.3m AEC-ABLE Deployable Articulated Mast boom (ADAM) constructed from graphite composite and steel cable was cantilevered off the side of the A/S, with 6 interface support struts between the boom and the spacecraft (Fig. 15). The principal objective of the IPEX-II experiment is to quantify the microdynamic stability of a potential structural element of the SIM structure. As in the case of IPEX-I, the prime concern is the existence of thermally induced snapping. A secondary objective is the determination of the dynamic properties of the boom on-orbit.



**Figure 15. IPEX-II Boom Flight Configuration**

To meet these objectives, the instrumentation included 24 micro-g Sundstrand QA200 accelerometers, 8 load cells, 42 temperature sensors, and 2 proof-mass shakers. A set of 6 accelerometers and 6 load cells were collocated inside the boom-to-spacecraft interface Struts to characterize the 6 interface degrees-of-freedom. Sixteen accelerometers were installed along the boom, including 2 that were collocated with the 2 shakers and load cells at the tip of the boom. The shakers performed on-orbit modal tests to characterize the linearity and modal properties of the boom. The remaining 2 accelerometers were installed on the A/S to detect the source of the vibrations measured on the boom. The 48 temperature sensors were installed on the IPEX-II boom, of which 24 were inside the accelerometer casing for calibration purposes, 22 were collocated with the accelerometers to monitor the ambient temperature in the event of a thermal snap, and 2 were on either side of a boom strut to investigate thermal gradients across a structural member.

Over 40 hours of on-orbit data was recorded. This included A/S nominal operations sequences, over 25 solar transitions, 12 modal experiments, and a 3mn period during which ALL systems including the gyros and the thrusters were turned off over a sun-bade transition, and a 10mn period during which the thrusters were activated in a particular set of sequences. The latter will be used to investigate the propagation of mechanical disturbances through the structure. The on-orbit tests will be followed by a suite of ground experiments and analyses performed at JPL, MIT and the University of Colorado at Boulder.

### 4. CONCLUSION

The IPEX-I experiment demonstrated the thermo mechanical stability of the ASTRO-SPAS platform on-orbit. Two full orbits of data were recorded. The [0-372 Hz] broadband mechanical disturbances were very low and approximately 150  $\mu$ g RMS at structural nodes with the thrusters turned off. The RMS is 15  $\mu$ g below 10 Hz. The powering up of the thrusters increased the RMS disturbance by 90  $\mu$ g RMS in the vicinity of the thrusters, but had little effect at distant locations, thus demonstrating the attenuation of the mechanical disturbances. Furthermore, it is the banging of the thruster mechanical relays which causes the increase in the disturbance levels, and not the actual pulsing of the gas. The gyros were also identified as predominant dynamic disturbances. Ground tests suggests that the measured gyro mode was aliased down from 800Hz to 55 Hz, and resulted in increases of 40  $\mu$ g RMS. Recent advances in thruster and gyro technology would significantly reduce these major disturbance sources on the A/S. At the structural nodes peak accelerations were less than 1 mg when the thrusters were off and less than 10mg when the thrusters were active, except for a single event on Channel 3 which recorded over 25mg. A residual motion analysis identified a 300 Hz bandwidth controller would be needed during nominal thruster operations to attenuate the motion down to 10nm, as required for SIM. Dynamic effects of the IMAPS telescope grating were also identified. No thermal snapping was observed in the data, although one isolated impulse was recorded and remains unexplained.

The dynamic environment of the A/S measured during the IPEX-I was used to design the follow-on IPEX-II experiment. The objective of IPEX-II is to characterize the microdynamic behavior and thermal mechanical stability of a representative SIM structural appendage. Preliminary data indicates that all the instrumentation functioned as planned during the flight.

### 5. REFERENCES

- [1]. Blair, M., and J. Sills, "Hubble Space Telescope On-Orbit System Identification", Proc. of the 12<sup>th</sup> International Modal Analysis Conf., Honolulu, Ha, Feb 1994, p. 663-669.
- [2]. Eilers, D., U. Lubbers, and F. De Rose, "EURECA-MMS Microgravity Measurement Subsystem Post-Flight Evaluation, Final Report", ESA/ESTEC Contract report NO. 10016, Bremen Germany, Dec. 1994.
- [3]. Levine, M., and R. Bruno, "Interferometry Program Experiment #1: Flight Data Analysis", NASA Jet Propulsion Laboratory Document JPL D-14904, Oct. 1997, Pasadena CA.
- [4]. H. Gutierrez and M. Levine, "Analysis of IPEX-2 Pre-Flight Ground Integration Test Data", NASA Jet Propulsion Laboratory Document JPL D-14905, Oct. 1997, Pasadena CA.